Converting Oil Shale to Liquid Fuels: Energy Inputs and Greenhouse Gas Emissions of the Shell in Situ Conversion Process

ADAM R. BRANDT*

Energy and Resources Group, 310 Barrows Hall, University of California at Berkeley, Berkeley, California 94720-3050

Received February 21, 2008. Revised manuscript received July 11, 2008. Accepted July 22, 2008.

Oil shale is a sedimentary rock that contains kerogen, a fossil organic material. Kerogen can be heated to produce oil and gas (retorted). This has traditionally been a CO_2-intensive process. In this paper, the Shell in situ conversion process (ICP), which is a novel method of retorting oil shale in place, is analyzed. The ICP utilizes electricity to heat the underground shale over a period of 2 years. Hydrocarbons are produced using conventional oil production techniques, leaving shale oil coke within the formation. The energy inputs and outputs from the ICP, as applied to oil shales of the Green River formation, are modeled. Using these energy inputs, the greenhouse gas (GHG) emissions from the ICP are calculated and are compared to emissions from conventional petroleum. Energy outputs (as refined liquid fuel) are 1.2−1.6 times greater than the total primary energy inputs to the process. In the absence of capturing CO_2 generated from electricity produced to fuel the process, well-to-pump GHG emissions are in the range of 30.6−37.1 grams of carbon equivalent per megajoule of liquid fuel produced. These full-fuel-cycle emissions are 21%−47% larger than those from conventionally produced petroleum-based fuels.

Introduction

The future of our liquid fuel supply is uncertain. Poor knowledge of petroleum resources, unavailable data, and varying definitions of reserves create disagreement about conventional oil availability (*1, 2*). In addition, we do not know which substitutes for conventional oil will be adopted after the peak in conventional oil production. Possible substitutes include nonconventional petroleum resources, other fossil fuels, or biological feedstocks. There is also disagreement about future liquid fuel demand: some predict future transportation systems based on energy carriers such as hydrogen or electricity (*3*), whereas others are not so sure (*4*). Because the greenhouse gas (GHG) impacts of these fuels differ, these variables contribute to uncertainty about future climate impacts (*5*).

Despite these uncertainties, one aspect of this problem is clear: a transition to hydrocarbon (HC) substitutes for conventional oil is already underway (*6, 7*). Oil shale is one of these resources (*8*). It is abundant and it occurs in regions with a heavy dependence on imported oil (e.g., the United States and China), making it appealing for strategic reasons (*9*). Unfortunately, oil shale production entails a heavy environmental burden, with traditional methods of production emitting high levels of criteria air pollutants, GHGs, and water pollutants (*10, 11*).

Oil shale is a sedimentary rock that contains fossil organic matter called kerogen. Kerogen is thought to be the source material from which naturally occurring oil and gas were formed, and thus oil shale is an "immature" oil source rock (*12*). The oil shale deposits of the Green River formation of Colorado, Utah, and Wyoming comprise approximately half of all known oil shale resources, or ~1500 gigabarrels (Gbbl) of oil equivalent (*12*). Green River oil shales contain between 5% and 40% kerogen by weight, with the higher end of this range being rare (*13*).

Hydrocarbons are generated from kerogen by heating it in an anoxic environment. Kerogen decomposes into a mixture of oil, HC gas, and carbon-rich shale coke that adheres to shale particles (as well as CO_2, water vapor, and trace gases). Kerogen decomposition rates are dependent on temperature: 90% decomposition occurs within 5000 min at 370 °C and within 2 min at 500 °C [see ref *13*, p 56]. Shale quality is quantified by the oil yield that results from the Fischer Assay (FA), which is often reported in terms of gal/ton. (The FA involves heating the shale to 500 °C at a rate of 12 °C/min and holding it at that temperature for 20 min (*13*). The oil produced from any retorting process may be different from the FA yield.) For a 26.7 gal/ton shale, the FA yield is 84% oil, 6% gas, and 10% char, by higher heating value (HHV) [see ref *13*, p 32].

There are two types of retorts: ex situ and in situ. Ex situ processes occur above ground and require the shale to be mined before it is processed. In situ processes apply heat to shale without removing it from the earth. Historical oil shale operations have largely been ex situ operations, whereas in situ processes are under active development (*8*). Recent oil shale research and development in the United States has been spurred by federal support for oil shale development (*14*). Of particular importance to this paper are three 160-acre federal leases won by Shell Frontier Oil and Gas, Inc. (hereafter referenced as Shell), through a Bureau of Land Management research and development program. All three of these leases are in western Colorado, and all will use the Shell in situ conversion process (ICP), which is a highly novel approach to in situ retorting.

This introduction is concluded by describing the ICP. Next, the method of modeling two ICP implementations is outlined. My results are then presented and discussed using two metrics: energy inputs and outputs per tonne of shale processed, and GHG emissions per megajoule (MJ) of refined fuel delivered (RFD).

A. Background: The in Situ Conversion Process. The ICP consists of four main steps. First, a freeze wall is created around the perimeter of an area of shale to be retorted (a production "cell"). Next, the oil shale within the cell is heated using electric resistance heating. The heat conducts through the formation, slowly heating the shale to the temperature of kerogen decomposition. After kerogen conversion, the resulting HCs are pumped from the earth. Lastly, the production cell undergoes remediation: residual mobile HCs are flushed from the earth and the freeze wall is thawed.

Both cases modeled in this paper are commercial-scale implementations of the ICP, but they are based on the Oil Shale Test (OST) Project, which is a subcommercial-scale test of the ICP that has been documented in detail in regulatory documents (*15, 16*). The ICP is also documented in tens of thousands of pages of patents. These patents are not generally useful for reconstructing the details of any

* Tel.: +1 510 847.9961. E-mail: abrandt@berkeley.edu.

10.1021/es800531f CCC: $40.75
Published on Web 08/23/2008

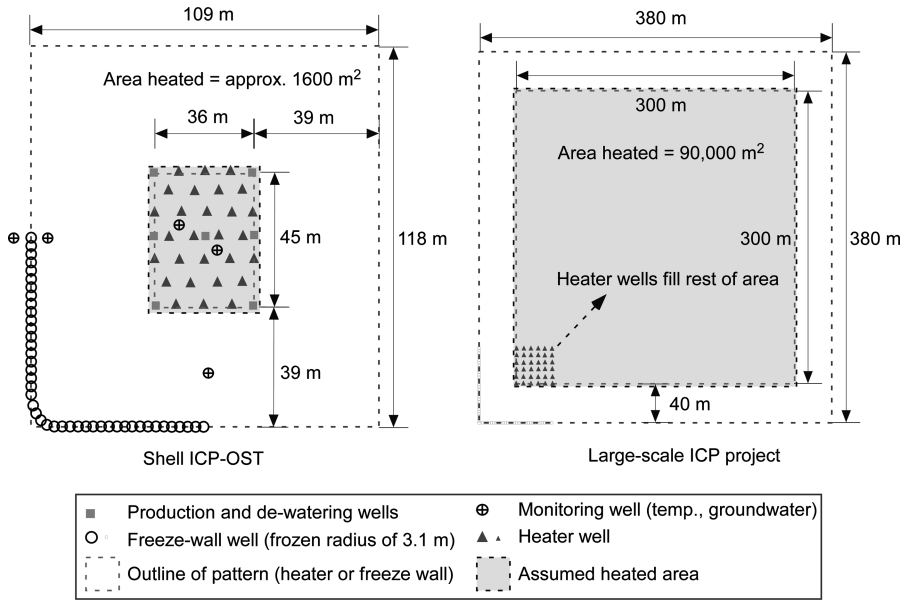

FIGURE 1. Well schematics for two configurations of the Shell in situ conversion process (ICP): Oil Shale Test (OST) (left) and two modeled cases (right). Heated area extends somewhat beyond heater well pattern. Not all monitoring wells are shown.

specific embodiment of the ICP: they describe multiple incarnations of the ICP, with data fragmented across many patents. The ICP now will be described in more detail.

1. Siting and Preliminary Operations. Production sites are chosen that contain a thick shale formation with low-permeability layers on the top and bottom. At the OST site, the shale lies under 270 m of inert overburden and is 320 m thick (*15*).

The layout of production cells in both the OST and in my two cases are shown in Figure 1. Larger cells are more efficient: the perimeter per volume of shale retorted is significantly smaller in larger cells, reducing heat waste and reducing freeze wall energy expenditure. It is unclear how large cells will be made in practice, given that the surface topography and subsurface heterogeneity might limit the size of cells (e.g., faults). Given the density of drilling required by the ICP, the land disturbance within a cell is profound. However, the thickness of the oil shale resource limits the amount of land disturbed per unit of energy produced.

2. Freeze Wall Construction. A single ring of wells is drilled around the cell. Refrigerant is circulated through internal and external well casing at approximately −40 °C (*15*). This forms an underground vertical wall of frozen soil and rock over a period of 1.5−2 years. In the OST, the final wall is 3.1 m thick, and the wells are placed at intervals of 2.5 m [see ref *15*, p 4-8]. If a cooler working fluid is used, the freeze wall will be thicker after it stabilizes, which would allow the wells to be drilled further apart [see *17*, p 394].

The freeze wall is maintained throughout the life of the project, extending in the OST 6.5 years [see ref *16*, p 3-16] to 8 years (*15*) after formation. The lower-permeability layers above and below the retorted shale act with the freeze wall to isolate the cell (*15*). This isolation is intended to keep produced HCs from escaping from the cell and to prevent additional groundwater from infiltrating the cell.

3. Water Removal. All shale porosity and fractures are initially filled with water (*16*). Wells are drilled in the cell interior to remove mobile water. Because water has a heat capacity four times that of shale, efficiency requires the removal of as much water as possible (*13*). After all drainable water has been removed, water will occupy ∼7% of cell bulk volume [see ref *16*, Appendix 21].

4. Heating. Heater wells are drilled at close spacing (7.8 m in the OST) in the cell and electric heaters are inserted into the wells. The spacing of heater wells is a tradeoff: closer well spacing allows the shale to be heated more quickly but increases drilling costs (*18*). These heaters heat the oil shale to temperatures of 340−400 °C (*15*).

The rate of heating can vary, and the temperature at which oil generation is complete decreases as the rate of heating slows. Therefore, it is more thermally efficient to heat the shale slowly (*18, 19*). At atmospheric pressure and a 3 °C increase per month, kerogen conversion is essentially complete at 300 °C, while at a 3 °C increase per day, conversion is not complete until 350 °C (*18, 19*). The rate of heating in the OST is ∼0.5 °C per day (∼350 °C increase over a two-year period).

The ICP converts kerogen to HCs at elevated pressures. Pore pressure during conversion is determined by the balance between the pressure generated by the vaporization of produced HCs and the pressure relieved as these products are removed by production wells (*20*). As an upper limit, pore pressure cannot exceed the lithostatic pressure (pressure applied to pore space from the overlying formation), because this would cause undesirable fracturing of the formation. One cited pressure range is between ∼0.2 MPa and ∼3.5 MPa (*17*).

Heat loss to the overburden is relatively small. Shell models project a temperature increase of 17 °C at a point 16 m above the top of the heated layer at the conclusion of heating [see ref *16*, Appendix 16, p 32]. This figure is consistent with results from my models (described below).

Heating also occurs outside of the perimeter of the heater-well pattern. Some of this heat results in kerogen conversion and some is wasted. In models of the OST, conversion is predicted 3−5 m outside of pattern after 900 days [see ref *16*, Appendix 22, p 10]. Waste heating begins beyond this point and extends toward the freeze wall. The freeze wall is placed so that energy from the heater wells will not appreciably reach it (*15*).

5. Recoverable Oil in Place. The amount and type of HCs produced from the ICP are uncertain, and published figures are in some disagreement (*18*). Oil yield is lower if the retorting is done slowly, at low temperature, or at higher pressure (*13, 18*). The ICP has all of these characteristics. Oil yields of 80 vol % of FA yield were found, given an ICP-like heating rate and atmospheric pressure, and yields as low as 60% occur at higher pressures [see ref *17*, Figure 197]. From test plots, Shell reports oil yields of ∼66% of FA oil yield (*15*).

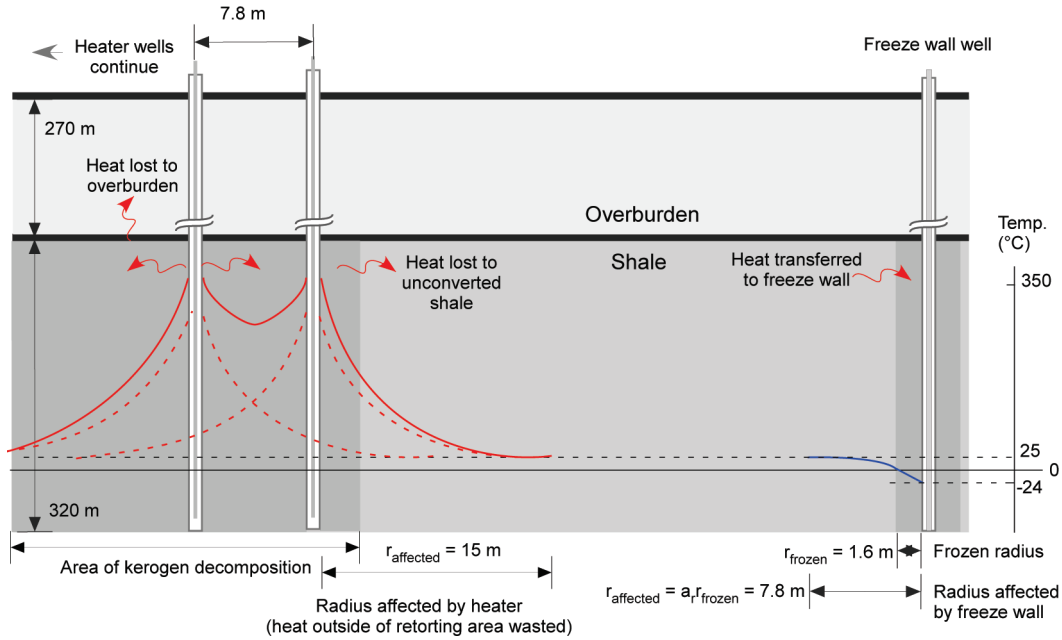

FIGURE 2. Illustrative temperature profiles in ICP. The radius that is affected by the heater well is shown at the time that the heater well was shut off. Horizontal scale is proportional to actual distances.

In the FA, ~7% of the total energetic yield is gas, with the remainder being oil and char. Slow, high-pressure heating such as that in the ICP process results in the production of more gas (*21, 22*), although published data are sparse.

Lastly, Shell does not state if their yield figures represent oil *generated* or oil actually *produced* from the well bore. The oil that is generated travels to production wells in the vapor phase, which reduces the potential for trapping (*16, 20*). However, oil flushed from the heated area can move toward the perimeter, instead of toward production wells (pressure gradients force some oil outward, where it condenses and is trapped through capillary mechanisms) [see ref *16*, Appendix 22]. It is this oil that the remediation process attempts to clean up.

6. Production. Long-chain, heavy HCs remain in the formation or are cracked. HCs travel toward the production wells in vapor form [see ref *17*, Column 241]. In the OST, the resulting HCs are pumped from the earth as liquid at a temperature of ~200 °C, using standard oil production techniques (*15*).

7. Restoration and Remediation. After oil production ceases, the production cell is flushed with water to recover any remaining mobile HCs and meet water quality standards [see ref *15*, p 5-1]. (Some HCs will remain, trapped in an largely immobile state in rock pores.) Shell claims that contaminant concentrations will decrease to allowable limits after flushing with 20 pore volumes of water [see ref *16*, p 11-11]. After the water quality targets are met, the freeze wall is allowed to thaw.

8. Upgrading and Refining. Oil from the OST requires pretransport desalting and minor distillation to reduce the vapor pressure [see ref *15*, p 4-18]. The ICP shale oil might also require upgrading before transport, because oil produced from ex situ retorts commonly does require upgrading (*9*). It is then sent to a refinery for conversion to finished fuel products. The synthetic crude oil produced is high-quality, with a high H:C ratio of ~1.9:1 [see ref *17*, Figure 180]. Thus, refining the synthetic crude oil will require less hydrogen input than refining a typical crude oil.

2. Methods

Two commercial-scale cases of ICP deployment, representing low and high energy and GHG intensity (hereafter the "low" and "high" cases), are modeled. Calculations of material and energy inputs and outputs are made in a life cycle assessment (LCA) framework, and GHG emissions are calculated for each case. Some site-specific data (e.g., total and effective porosity) are taken from Shell reports without the possibility of independent verification. This necessarily leads to some uncertainty in these results.

A. Life Cycle Assessment. A simplified LCA is performed for each case, using a process-model approach (*23*). Low and high cases use plausible low and high estimates for inputs (e.g., steel input), energy intensity of each input (e.g., embodied energy per unit of steel), and yields of oil and gas. A conscious effort was made to choose conservative (low) values for inputs and energy intensities. Methods for important LCA stages are described below. See Supporting Information for more details.

1. Freeze Wall Construction. The numbers of the wells drilled and their depths are taken from the OST [see ref *15*, Exhibits L, N], scaled to commercial cell size (see Figure 1). A casing temperature of −40 °C is assumed over the length of the wall after stabilization. Freeze wall energy requirements are modeled using the technique of Sanger and Sayles (*24*). The resulting freeze wall temperature profile (along with simplified heater well profiles) is given in Figure 2.

After the wall is complete, heat conducted through the completed wall is removed over the lifetime of the project (*15*). Energy transfer through the completed wall is modeled with one-dimensional (1-D) steady-state heat conduction (*25*). Energy transfer occurs from the edge of wall at 0 °C to the center of the wall at an averaged axis temperature (*24*). Refrigeration efficiency is calculated using input and output temperatures (*26*). The calculated coefficient of performance (COP) is 2.7 for the high case. For the low case, a higher COP value of 3.5 is assumed.

The energy consumed in maintenance of the freeze wall over the life of the project is significantly in excess of the energy required to initially freeze the wall (approximately an order of magnitude larger). Also, the calculations include the removal of sensible heat outside of the freeze wall, avoiding errors that result from neglecting this factor [see ref *24*, p 315].

2. Heating. Heating occurs until the average bulk shale temperature reaches the calculated conversion temperature,

TABLE 1. Primary Energy Inputs and Outputs per Tonne of Shale Processed (MJ/tonne) and Energy Ratios[a]

		energy per tonne of shale produced (MJ/tonne)			
		low case		high case	
	type of energy input (I or E)[b]	input	output	input	output
	Production Site Inputs				
1. Preliminary operations	E	1		1	
2. Drilling	E	7		12	
3. Miscellaneous	E	34		34	
4. Pumping	E	2		4	
5. Freeze wall, purchased electricity	E	37		159	
6. Freeze wall, generated electricity	I	35			
7. Retorting, purchased electricity	E			570	
8. Retorting, generated electricity	I	1154		784	
9. Remediation, purchased electricity	E			74	
10. Remediation, generated electricity	I	39			
	Production Site Output				
11. Synthetic crude oil			2632		2543
	Offsite Inputs				
12. Crude transport, electricity	E	2	13		
13. Refining, external energy input	E	56	83		
14. Refining, internal energy input	I	157	230		
15. Refined product transport	E	16	16		
	Net Output Offsite				
16. Refined fuel delivered, RFD			2475		2333
	Energy Ratios				
EER[c]			15.8		2.4
NER[d]			1.6		1.2
NER, if gas is exported[e]			2.5		1.6
NER, crude production only[f]			2.0		1.6

[a] All electricity converted to primary energy quantities using efficiencies from the text. [b] I = internal energy inputs, E = external energy inputs. [c] Using line numbers, EER = 16/(1 + 2 + 3 + 4 + 5 + 7 + 9 + 12 + 13 + 15). [d] NER = 16/(1 + 2 + 3 + 4 + 5 + 6 + 7 + 8 + 9 + 10 + 12 + 13 + 14 + 15). [e] Here, produced HC gas is added to the numerator (i.e., we assume the project exports produced gas), and electricity is purchased to replace it. [f] For crude production only, NER = 11/(1 + 2 + 3 + 4 + 5 + 6 + 7 + 8 + 9 + 10).

at which time heating ceases and subsequent heat transfer is ignored. The geothermal gradient results in an average initial shale temperature of 29 °C [see ref *16*, Appendix 16, p 15].

Oil generation from kerogen is modeled as a first-order reaction (*27, 28*). The ICP requires a nonisothermal first-order model, such as that from Campbell et al. (*27*) In this model, the shale undergoes a constant temperature change per unit time, which is a good approximation of the ICP heating rate of 0.5 °C/day (*15, 17*). Using the Campbell model at these heating rates, oil generation should be complete at 330 °C. Unfortunately, this model does not account for the fact that increased pressure inhibits the distillation of generated HCs out of the source rock, thereby reducing the oil yield, because of increased coking and cracking (*22*). For example, at ~2.7 MPa and a heating rate of 1 °C/h, the model predicts complete conversion at a temperature that is ~25 °C too low (*22*). Instead of using the much more complex model of kerogen decomposition that was later developed for use with arbitrary temperature-pressure histories (*29*), Campbell's model (with a 10−30 °C penalty due to pressure) is used. Thus, in this model, complete kerogen conversion occurs at 340 and 360 °C in the low and high cases, respectively.

The energy requirement for heating is given by the heat (or enthalpy) of retorting, linearly interpolated from published figures (*13, 30*). The enthalpy of retorting is adjusted for the residual water content of shale, assuming no influx of water from leaks in the containment system. At these temperatures, the interpolated enthalpies of retorting are 414 and 446 MJ/tonne without water adjustment (low and high, respectively) and 473 and 495 MJ/tonne (low and high, respectively) after water adjustment.

Heat losses to the overburden and underburden and perimeter are also included. Temperature, as a function of distance, is modeled as radial heat conduction through a solid from multiple sources (see Supporting Information). Because of the low porosity of unretorted shale, convective heat transfer before retorting is likely to be small (this is conservative: convective heat transfer would "smear out" the temperature distribution and result in additional heat being wasted). Heat loss to the overburden and underburden adds 3% to the heating energy requirement, and perimeter heat loss adds somewhat less than 7%.

3. Electricity Generation. Co-produced HC gas is burned on-site in a combined-cycle natural gas turbine with 45% efficiency. Remaining demand is met with external electricity. Electricity imports in the high case are from the mix of plants generating in Colorado (~72% coal and ~24% natural gas in 2005) (*31*), with an efficiency of generation and transmission of 33%. In the low case, electricity imports are provided by combined cycle natural gas turbines with 45% efficiency (*32*).

4. Recoverable Oil in Place. Recoverable oil in place is calculated using the depth of the oil shale resource multiplied by the heated area (*15*), assuming an average richness of 26.5 gal/ton (110.4 L/tonne) (*13*). The heated area is increased by 3 m in each direction, to account for retorting outside of the heater well pattern.

I assume pressures of 0.8 and 1 MPa (low and high cases, respectively). (See Supporting Information for discussion.) Liquid yields are 64% (low) and 67% (high) of FA yield at my assumed pressures and temperatures of completion (the

lower yield is associated with higher temperatures and pressures) (*17*). In the high and low cases, 90% and 97.5% recovery of generated oil, respectively, is assumed.

Shell data from a test project suggest that the gas yield is 32% of the total energetic yield [see ref *33*, p 14]. This gas yield is used for our low case. However, these gas yields are higher than any reported in the public literature. A reason for this high gas yield could be that shale near heater wells is heated to temperatures above those required for oil generation. Methane and hydrogen continue to evolve at higher temperatures (one study found that gas evolution did not peak until more than 95% of the oil had been generated (*34*)). Therefore, for the high case, we use gas yields from independent data at the closest heating rate and pressure to the ICP process (*22*). After adjusting for discrepancies in those data, the reported gas yield is 21% of the total yield.

Using these data, the energetic yields per tonne, in the low and high cases, are 2755 MJ oil and 1285 MJ gas, and 2543 MJ oil and 784 MJ gas, respectively. The large uncertainty in gas yield significantly affects the energy ratios for the two processes.

5. Refining. Here, refining has been modeled in a simple fashion, to allow comparison with other estimates of well-to-wheels (WTW) GHG emissions (e.g., the GREET WTW emissions estimates described by Wang et al. (*35*)). Shale oil is converted completely to a generic "refined liquid fuel". Here, 2005 input−output data from U.S. refineries is used to calculate energy efficiency and the external and internal energy inputs ($\eta = 0.89$; see Supporting Information). Because the synthetic crude oil produced has a high hydrogen content, a 33% reduction in energy consumption in the refinery was assumed in the low case [see ref *17*, Figure 180].

All calculations and figures are given in terms of megajoules of refined fuel delivered (MJ RFD). Refined fuel delivered is a composite energy good that represents the net energy output from the refinery as fuel suitable for end-use consumption (gasoline, diesel, jet fuel, etc.).

B. Comparison of Energy Inputs and Outputs. Using the results from the LCA, two energy ratios can be computed: the external energy ratio (EER) and the net energy ratio (NER) (*36*).

$$\mathrm{EER} = \frac{E_{\mathrm{out}}}{E_{\mathrm{ext}}} \tag{1}$$

$$\mathrm{NER} = \frac{E_{\mathrm{out}}}{E_{\mathrm{ext}} + E_{\mathrm{int}}} \tag{2}$$

Here, E_{out} is the HHV of the final refined product output, E_{ext} the primary energy input from the outside energy system (such as electricity purchased from the grid), and E_{int} the primary energy input from the feedstock resource itself (e.g., electricity generated from co-produced HC gas). The EER compares energy inputs from outside the system to net outputs from the process. It reflects the ability of the process to increase the energy supply to society. The NER compares *all* energy inputs to net outputs. Therefore, it is a better metric for understanding impacts from producing a fuel (e.g., GHGs) (*36*).

1. Emissions. Energy inputs to each process step (expressed in terms of MJ/MJ RFD) are multiplied by the emissions factor for the fuel consumed in that step, giving the number of grams of carbon equivalent GHGs per megajoule of refined fuel delivered ($g_{C_{equiv}}$/MJ RFD). The fuel used in some steps is unclear or not cited, which requires assumptions. In addition, fugitive GHG emissions from production operations were added (*37*).

Results

A. Energy Inputs and Outputs per Tonne of Shale Processed. The primary results from the previously described calculations are presented in Table 1 for both of my cases.

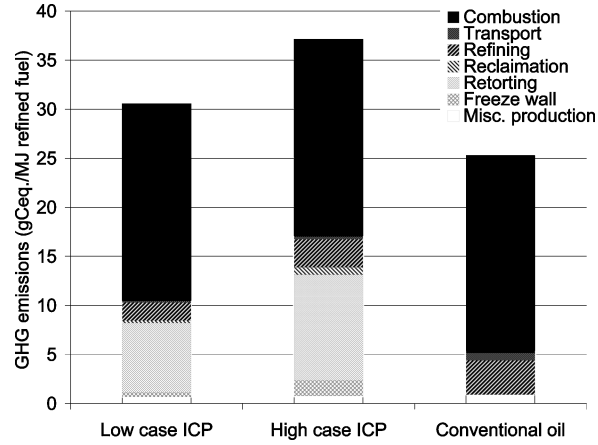

FIGURE 3. Full-fuel-cycle emissions from low and high primary cases, grams of carbon equivalent per megajoule of refined fuel delivered ($g_{C_{equiv}}$/MJ RFD), as compared to conventional oil emissions (*39*).

In the table, "I" designates an internal energy input and "E" designates an external energy input. Energy ratios (EER and NER) are also presented in Table 1. In the low case, the EER and NER are quite different. This is because of the large amount of co-produced HC gas that is used to fuel the process itself. In the high case, the EER is much lower, because less gas is produced and the energy inputs are greater. The NER is much lower for these two processes, but it is still above unity.

Table 1 also shows the NER if the produced gas is sold and electricity is purchased in its place. In this case, no changes are made to total energy consumption, only the system boundaries are adjusted. This illustrates a difficulty of energy ratios: they are sensitive to essentially arbitrary system boundary definitions (*36*). We also show the NER of the crude oil production step only. Shell states that 3−3.5 times as much energy is produced as crude oil as is used by the heaters. (*38*) My result is lower because their figure includes only heaters, not other inputs, and also because their figure assumes 60% efficient natural gas electricity generation, compared to my assumption of 45% efficient generation plus transmission (*38*).

B. Emissions per Unit of Final Fuel Delivered. Full fuel-cycle emissions per MJ RFD are plotted in Figure 3. The summaries of the total emissions are 30.6 and 37.1 $g_{C_{equiv}}$/MJ RFD in the low and high cases, respectively. Additional results are given in the Supporting Information. Fugitive emissions are added to the miscellaneous production category. For comparison, emissions from conventionally produced fuels are presented (the average of gasoline and diesel is 25.3 $g_{C_{equiv}}$/MJ). (*39*) Note that if electricity were generated from low-carbon sources (such as renewables or fossil fuels with carbon capture), then emissions from oil shale would be approximately equal to those from conventional oil. Emissions from final fuel combustion are equal in all cases, because the fuels that are produced from oil shale are equivalent to those from conventional petroleum.

C. Comparison to Other Greenhouse Gas (GHG) Emissions Estimates. Burnham and McConaghy studied the ICP (*18*). Their emissions estimates are ∼27−34 $g_{C_{equiv}}$/MJ of FFD, although their treatment of co-produced natural gas seems to differ from the treatment [see ref *18*, p 6]. An early oil shale emissions estimate put wide bounds on emissions from surface retorting of 25 gal/ton oil shale (*11*). These emissions estimates were in the range of 31−74 $g_{C_{equiv}}$/MJ. The emissions estimates in this report also can be compared to those from other substitutes for conventional petroleum: emissions from Alberta tar sands production are in the range of 29−36 $g_{C_{equiv}}$/

MJ, whereas those from coal-based synthetic fuels are in the range of 42−49 $g_{C_{equiv}}$/MJ. (*5*)

D. Large-Scale and Long-Term Emissions Impacts. Near-term emissions from the ICP are likely to be closer to the high estimate presented in this report. Conservative estimates of the required inputs were made in this report. Also, near-term development may be fueled with the existing grid, which is more carbon-intensive than co-produced electricity. Also, formations may not be converted fully as this report assumes, but, instead, in sections. (This was suggested in recent Shell documents (*16*), and this would increase perimeter-dependent inputs.) Lastly, early incarnations of technologies are never fully optimized.

In the long term, it is possible to implement a low-carbon ICP. The energy requirements of heating are likely to not be sensitive to intermittency, because of the high heat capacity of the large mass of shale and the long heating time. Thus, intermittent renewables could be used in off-peak times. Second, the reuse of waste heat seems feasible, given that the hot, depleted production cells will need be flushed with water to meet the water quality requirements in any case. However, these low-carbon ICP options are costly and, therefore, are unlikely without regulation of carbon emissions.

Large-scale oil shale development could result in significant additional emissions. If we produce, refine, and combust fuel equal to 10% of the 2005 U.S. gasoline consumption (∼1.8×10^{18} J) (*40*), using the ICP instead of conventional oil, full-fuel cycle emissions increase from ∼45 million tonnes of carbon (MtC) for conventional oil to 55−67 MtC. This approximate increase of 10−20 MtC can be compared to total emissions from the state of Colorado, which were 24 MtC in 2001 (*41*).

The wide range of potential impacts of the ICP and its inherent flexibility underscore the importance of deliberately and consciously choosing our path as we transition to oil substitutes (*6*). Finding an environmentally responsible path to secure domestic fuel supplies will be dependent not only on developing new alternatives to oil, but also on implementing policies and programs to guide the responsible deployment of these technologies.

Acknowledgments

Alan Burnham generously provided much helpful assistance with this work. Roger Bailey also provided helpful advice. James Bartis, Ralph Coates, Richard Plevin, and Alex Farrell provided feedback. Funding for a previous incarnation of this research was provided by the Natural Resources Defense Council.

Supporting Information Available

Document includes additional methodological details, outlined by production stage, as well as one additional figure and additional results in two tables (12-page PDF). This material is available free of charge via the Internet at http://pubs.acs.org.

Literature Cited

(1) Bentley, R. W. Global oil & gas depletion: an overview. *Energy Policy* **2002**, *30* (3), 189–205.
(2) Yergin, D. Hearing on Global Energy Security Issues, Testimony of Dr. Daniel Yergin. United States Senate Committee on Foreign Relations, Subcommittee on International Economic Policy, Export and Trade Promotion, Washington, DC, 2003.
(3) Sperling, D.; Ogden, J. M. The Hope for Hydrogen. *Issues Sci. Technol.* **2004**, *2004* (Spring), 1–8.
(4) Romm, J. The Hype About Hydrogen. *Issues Sci. Technol.* **2004**, *2004* (Spring), 1–8.
(5) Brandt, A. R.; Farrell, A. E. Scraping the bottom of the barrel: CO_2 emission consequences of a transition to low-quality and synthetic petroleum resources. *Climatic Change* **2007**, *84* (3−4), 241–263.
(6) Farrell, A. E.; Brandt, A. R. Risks of the oil transition. *Environ. Res. Lett.* **2006**, *1*, (1).
(7) Greene, D. L.; Hopson, J. L.; Li, J. Have we run out of oil yet? Oil peaking analysis from an optimist's perspective. *Energy Policy* **2006**, *34*, 515–531.
(8) Bartis, J. T.; LaTourrette, T.; Dixon, L.; Peterson, D. J.; Cecchine, G. *Oil Shale Development in the United States: Prospects and Policy Issues*; RAND: Santa Monica, CA, 2005; p 68.
(9) Johnson, H. R.; Crawford, P. M.; Bunger, J. W. *Strategic Significance of America's Oil Shale Resource: Volume I—Assessment of Strategic Issues*; AOC Petroleum Support Services, LLC: Washington, DC, March 2004; p 45.
(10) *An Assessment of Oil Shale Technologies*; Congress of the United States, Office of Technology Assessment (OTA): Washington, DC, 1980; Vol. 1, p 517.
(11) Sundquist, E. T.; Miller, G. A. Oil shales and carbon dioxide. *Science* **1980**, *208* (4445), 740–741.
(12) Dyni, J. R. *Geology and resources of some world oil-shale deposits*; Paper No. 2005-5294; U.S. Geological Survey, U.S. Department of the Interior: Reston, VA, 2006, p *42*.
(13) Hendrickson, T. A. *Synthetic Fuels Data Handbook*; Cameron Engineers, Inc.: Denver, CO, 1975.
(14) BLM announces results of review of oil shale research nominations. Bureau of Land Management, 2006 (accessed 7/2006).
(15) Oil Shale Test Project, Oil Shale Research and Development Project. Plan of operation. Submitted to Bureau of Land Management, Shell Frontier Oil and Gas, Inc., 2006.
(16) Designated Mining Operation Reclamation Permit Application for the Shell Frontier Oil and Gas, Inc., Oil Shale Test Project; Colorado Division of Reclamation and Mining Safety, Department of Natural Resources: Denver, CO, 2007.
(17) Berchenko, I.; et al. In situ thermal processing of an oil shale formation using a pattern of heat sources. U.S. Patent 6991032 B2, January 31, 2006.
(18) Burnham, A. K.; McConaghy, J. R. *Comparison of the acceptability of various oil shale processes*; Report UCRL-CONF-226717; Lawrence Livermore National Laboratory: Livermore, CA, 2006.
(19) Burnham, A. K. *Chemical kinetics and oil shale process design*; Report UCRL-JC-114129; Lawrence Livermore National Laboratory, Livermore, CA, July 18−31, 1993.
(20) Burnham, A. K. Personal communication with Alan Burnham regarding oil shale production, 2007.
(21) Bae, J. H. Some effects of pressure on oil-shale retorting. *Soc. Pet. Eng. J.* **1969**, (September), 287–292.
(22) Burnham, A. K.; Singleton, M. F. High-Pressure Pyrolysis of Green River Oil Shale. In *Geochemistry and Chemistry of Oil Shales*; Miknis, F. P., McKay, J. F., Eds.; ACS Symposium Series 230; American Chemical Society: Washington, DC, 1983.
(23) Ciambrone, D. F. *Environmental Life Cycle Analysis*; Lewis Publishers: Boca Raton, FL, 1997.
(24) Sanger, F. J.; Sayles, F. H. Thermal and rheological computations for artificially frozen ground construction. *Eng. Geol.* **1979**, *13*, 311–377.
(25) Incropera, F. P.; Dewitt, D. P.; Bergman, T. L.; Lavine, A. S. *Fundamentals of Heat and Mass Transfer*; John Wiley and Sons: Hoboken, NJ, 2007.
(26) Stoecker, W. F. *Industrial Refrigeration Handbook*; McGraw−Hill: San Francisco, CA, 1998.
(27) Campbell, J. H.; Koskinas, G. H.; Stout, N. D. Kinetics of oil generation from Colorado oil shale. *Fuel* **1978**, *57* (6), 372–376.
(28) Shih, S. M.; Sohn, H. Y. Nonisothermal determination of the intrinsic kinetics of oil generation from oil shale. *Ind. Eng. Chem. Process. Des. Dev.* **1980**, *19* (3), 420–426.
(29) Burnham, A. K.; Braun, R. L. General kinetic model of oil shale pyrolysis. *In Situ* **1985**, *9* (1), 1–23.
(30) Sohns, H. W.; Mitchell, L. E.; Cox, R. J.; Barnet, W. I.; Murphy, W. I. R. Heat requirements for retorting oil shale. *Ind. Eng. Chem.* **1951**, *43* (1), 33–36.
(31) Electricity Net Generation: Total (All Sectors), 1949−2006 (Table 8.2a). In *Annual Energy Review 2006*; DOE/EIA-0384(2006); Energy Information Administration (EIA): Washington, DC, June 27, 2007.
(32) Spath, P. L.; Mann, M. K. *Life cycle assessment of a natural gas combined-cycle power generation system; NREL/TP-570−27715*; National Renewable Energy Laboratory: Golden, CO, September 2000; p 56.
(33) Vinegar, H. *Shell's In-situ conversion process*; National Academy of Sciences Earth Resources Committee: Washington, DC, 2006.
(34) Huss, E. B.; Burnham, A. K. Gas evolution during pyrolysis of various Colorado oil shales. *Fuel* **1982**, *61*, 1188–1196.

(35) Wang, M.; Lee, H.; Molburg, J. Allocation of energy use in petroleum refineries to petroleum products—Implications for life-cycle energy use and emission inventory of petroleum transportation fuels. *Int. J. Life Cycle Assess.* **2004**, *9* (1), 34–44.

(36) Spitzley, D. V.; Keoleian, G. *Life Cycle Environmental and Economic Assessment of Willow Biomass Electricity: A Comparison with Other Renewable and Non-Renewable Sources CSS04-05R*; University of Michigan: Ann Arbor, MI, March 25, 2004; p 76.

(37) *Inventory of U.S. greenhouse gas emissions and sinks: 1990–2005*; Environmental Protection Agency (EPA): Washington, DC, 2007.

(38) *Utah Heavy Oil Program A Technical, Economic, and Legal Assessment of North American Oil Shale, Oil Sands, and Heavy Oil Resources*; Institute for Clean and Secure Energy: Salt Lake City, UT, September 2007.

(39) Wang, M. Q. GREET Model 1.8a; Argonne National Laboratory: Argonne, IL, 2007.

(40) Consumption for Electricity Generation by Energy Source (Table 8.4a). In *Annual Energy Review 2006*; DOE/EIA-0384(2006); Energy Information Administration (EIA): Washington, DC, June 27, 2007.

(41) *State Carbon Dioxide Emissions*; Energy Information Administration (EIA): Washington, DC, (accessed 7/2006).

ES800531F